Optimal Capacity Expansion Planning with Multi-Terminal High Voltage DC Transmission

Jesse Holzer, Osten Anderson, Konstantinos Oikonomou, Patrick Maloney, Casey Burleyson, Marcelo Elizondo
(jesse.holzer; osten.anderson; konstantinos.oikonomou; patrick.maloney; casey.burleyson; marcelo.elizondo) @pnnl.gov
Pacific Northwest National Laboratory, Richland, WA, USA.

***Abstract*—With heightened focus on ensuring reliable and cost-effective grid operations during the integration of large electric loads, such as data centers, and inverter-based resources, it is crucial that capacity expansion planning (CEP) models include comprehensive transmission planning. High Voltage Direct Current (DC) transmission has advantages in reliability, controllability, and cost, but understanding the optimal location and sizing of these transmission investments remains a key challenge. This paper presents a novel CEP model that explicitly integrates multi-terminal DC (MTDC) transmission in long-term system planning. To capture the operational constraints and trade-offs between transmission technologies, (i.e., MTDC, point-to-point DC, AC) the model includes power flow physics on AC and DC networks, incorporates converter station investments, and enables dynamic selection of network configurations, including meshed and radial layouts. The model is applied to the Western Interconnection using a 43-zone system in a baseline scenario and with higher load growth from data centers. Results indicate, MTDC transmission can reduce total investment and operational costs by 4% and lower converter capacity needs through optimized network design and more efficient coordination of generation resources.**

***Index Terms*—capacity expansion planning, multi-terminal high voltage DC transmission.**

I. INTRODUCTION AND LITERATURE REVIEW

Multi-Terminal High Voltage Direct Current (MTDC) transmission is increasingly being considered by transmission planners as an alternative to both point-to-point High Voltage Direct Current (DC) and conventional High Voltage Alternating Current (AC). This trend reflects inherent advantages of MTDC in certain grid applications [1]–[3]. Compared to point-to-point DC lines, a radial MTDC needs fewer converters for the same locations of exchange with the AC grid, thus reducing capital costs. Also, its modular architecture enables staged transmission expansion, which is harder with point-to-point. Meshed MTDC systems, having parallel transmission paths, have the further advantage of improved reliability under failure due to alternate current paths, and they need even fewer converter stations. DC in general has significant advantages over AC for long-distance transmission, including lower capital cost, reduced losses, enhanced controllability of power flow, and reactive power support [4]. And DC and MTDC are seen as critical technologies for bolstering the transmission grid to meet the rapidly increasing power needs of data centers [5].

Realizing the advantages of MTDC systems over conventional transmission technologies requires accurate representation of MTDC in capacity expansion planning (CEP) models. CEP models determine cost-effective strategies for transmission and generation siting and sizing to meet long-term electricity demand. To capture the full value and limitations of MTDC, CEP models must enable the dynamic design of MTDC networks by independent selection and sizing of DC links and converters, and must include the physics of power flow in meshed AC and DC networks linked by converters.

Recent work in CEP modeling with both AC and DC systems falls into two categories, the first using on linear programming (LP) and mixed-integer (linear) programming (MIP), and the second using more complex methods like quadratic programming (QP) or nonlinear programming (NLP). MIP and especially LP solvers scale better on large systems, but QP and NLP models can represent system behavior more accurately. LP/MIP formulations for coordinated AC/DC planning are used in [6]–[10]. In [6], a hybrid AC/DC CEP model includes construction of new lines and conversion of existing AC lines to DC. In [7], a stochastic AC/DC CEP is solved with Benders decomposition, with subproblems for outages. In [8], hybrid AC/DC CEP formulations are extended by incorporating alternative control strategies for voltage source converters (VSCs). In [9], the AC/DC CEP is enhanced by a piecewise-linear loss model. [10] examines the effects of high-renewable-penetration scenarios on the scale and balance of AC and DC transmission investments. In [11], a QP AC/DC CEP captures voltage and reactive power with converter transformers, filters, and phase reactors. In [12], an NLP AC/DC CEP examines trade-offs between AC and DC for offshore wind integration, accounting for remedial action schemes.

Recent high profile CEP studies and packages, e.g., [13], [14], [15], [16], have considered investment in DC transmission capacity in fixed configurations, in fixed proportion with converter capacity, or have allowed independent sizing and selection of DC links and converters without accounting for the physics of power flow in the resulting synchronous networks of new and existing AC and DC lines.

This work fills this gap by presenting a novel, high-fidelity MIP formulation that explicitly represents point-to-point DC, AC, and radial and meshed MTDC networks in a CEP

This work is supported by the Energy System Co-Design with Multiple Objectives and Power Electronics (E-COMP) Initiative of the Pacific Northwest National Laboratory (PNNL). PNNL is operated by Battelle for the United States Department of Energy under Contract DE-AC05-76RL01830.

Corresponding author: jesse.holzer@pnnl.gov

979-8-3315-8138-1

framework. The model enables the dynamic design of the network configuration and accounts for the physics of power flow. Thus, the proposed CEP model competes MTDC against DC and AC investments more accurately than prior works.

The model is formulated in Section II. In section III, we apply the model to the U.S. Western Interconnection to quantify the long-term investment value of MTDC in a realistic large-scale system. The analysis explores alternative future scenarios, with and without additional load growth from large electric loads (LELs) such as data centers, thus addressing timely policy questions on transmission system development.

II. MTDC CEP Model Formulation

This section formulates the CEP optimization model, including new features for planning a mixed network of AC and DC lines and AC-DC converters in point-to-point and multi-terminal configurations. Other CEP features, e.g., storage and policy constraints, are modeled in the simulations but not described here as this work focuses on transmission modeling. Further details of the model formulation are in [17], [18].

Building on an established CEP formulation [17], [18], we add DC candidate lines and AC-DC converters to the existing and candidate AC network and add decoupled power flow (DCPF) constraints to represent the physics of power flow. These additions to the basic CEP are the main novel feature of our model. Candidate transmission projects are modeled as zone-to-zone links, enabling joint optimization of AC, point-to-point DC, and MTDC capacity and configuration. This approach allows the optimization solver to determine network topology by link selection and to economize on converter sizing for the topology, resulting in an optimal MTDC design.

Without the power flow laws, the model reduces to a transport flow formulation that considers only transmission capacities and investment costs, as used in many prior CEP studies. In transport flow, the multiple synchronous AC and DC networks connected by converters act as a single network. This can bias investment decisions toward options with low capital cost per unit of capacity, without accounting for congestion and network physics. Incorporating DCPF enforces physical power flow limits in meshed AC and MTDC networks, avoiding this bias and producing more realistic transmission and converter investments.

Adding DCPF improves physical accuracy but adds computational complexity. As first formulated, DCPF uses quadratic expressions that are hard for practical optimization solvers to handle at large scale. To address this, we restrict investment variables to binary values, enabling a linear reformulation of the DCPF. Binary investment is used in this work to capture the physics of DC and AC transmission, but it also is a natural way of modeling detailed project selection, as in [19].

A. Basic CEP Model

The basic CEP model is an LP that determines the optimal level and timing of investment in grid infrastructure (generation and transmission) as well as the operation of new and existing assets to serve load, minimizing total investment and operating costs.

We consider power grid geography with zones $n \in N$ (e.g., large spatial areas, or individual nodes of the grid), a time horizon of investment periods $y \in Y$ (e.g., years or decades), operational time points $t \in T$ (e.g., hours of selected days in a year), and infrastructure projects $i \in I$ including generation projects I^{gn} and transmission projects I^{tr}.

Each project i is characterized by the capacity P_i^{cap} of a representative unit, the investment cost C_i^{inv}, and the operating cost C_i^{gn} for $i \in I^{\text{gn}}$. Investment decisions are modeled by continuous variables u_{iy}^{inv} for the number of units of project i built and u_{iy}^{op} for the number operating in period y. Operational decisions use variables p_{iyt} for the power of project i in period y at time t, i.e., generation for $i \in I^{\text{gn}}$ and flow for $i \in I^{\text{tr}}$.

Projects are partitioned into existing projects I^{ex} and candidate projects I^{cand}. For $i \in I^{\text{cand}}$, based on the lifetime, capacity built in period y operates in periods in a set Y_{iy}^{fwd}, so u^{inv} determines u^{op} in (2). Candidate investment is bounded by resource limits in (3, 4). Existing project capacities are fixed in (5). Operational power is bounded by the operating capacity $P_i^{\text{cap}} u_{iy}^{\text{op}}$ in (6, 7), with availability (e.g., for variable generation) F_{iyt}^{avail} in (6). Project geography is an injection zone n_i^{inj} for $i \in I^{\text{gn}}$, and from and to zones n_i^{fr} and n_i^{to} for $i \in I^{\text{tr}}$. Load is a fixed value P_{nyt}^{ld}. Energy balance is enforced by (8), where $I_n^{\text{gn}} = \{i \in I^{\text{gn}} : n_i^{\text{inj}} = n\}$, $I_n^{\text{fr}} = \{i \in I^{\text{tr}} : n_i^{\text{fr}} = n\}$, and $I_n^{\text{to}} = \{i \in I^{\text{tr}} : n_i^{\text{to}} = n\}$. The objective is to minimize the total of investment and operational costs in (1), where the duration D_t converts hourly cost rates to costs.

$$\min \sum_{i \in I^{\text{cand}}, y \in Y} C_i^{\text{inv}} u_{iy}^{\text{inv}} + \sum_{i \in I^{\text{gn}}, y \in Y, t \in T} D_t C_i^{\text{gn}} p_{iyt} \tag{1}$$

$$u_{iy}^{\text{op}} = \sum\nolimits_{y' : y \in Y_{iy'}^{fwd}} u_{iy'}^{\text{inv}}, \forall i \in I^{\text{cand}}, y \in Y \tag{2}$$

$$0 \le u_{iy}^{\text{inv}} \le U_{iy}^{\text{inv,max}}, \forall i \in I^{\text{cand}}, y \in Y \tag{3}$$

$$0 \le u_{iy}^{\text{op}} \le U_{iy}^{\text{op,max}}, \forall i \in I^{\text{cand}}, y \in Y \tag{4}$$

$$u_{iy}^{\text{op}} = U_{iy}^{\text{ex,op}}, \forall i \in I^{\text{ex}}, y \in Y \tag{5}$$

$$0 \le p_{iyt} \le F_{iyt}^{\text{avail}} P_i^{\text{cap}} u_{iy}^{\text{op}}, \forall i \in I^{\text{gn}}, y \in Y, t \in T \tag{6}$$

$$-P_i^{\text{cap}} u_{iy}^{\text{op}} \le p_{iyt} \le P_i^{\text{cap}} u_{iy}^{\text{op}}, \forall i \in I^{\text{tr}}, y \in Y, t \in T \tag{7}$$

$$\sum\nolimits_{i \in I_n^{\text{gn}}} p_{iyt} + \sum\nolimits_{i \in I_n^{\text{to}}} p_{iyt} = \sum\nolimits_{i \in I_n^{\text{fr}}} p_{iyt} + P_{nyt}^{\text{ld}}, \quad \forall n \in N, y \in Y, t \in T \tag{8}$$

B. Construction of AC/DC Candidate Transmission Network

Next we specify the candidate transmission projects as AC or DC links or AC-DC converters, with DC zones, overlaid on a network of existing AC projects in AC zones. For AC zone n, create a DC zone n_n^{dc} collocated with n, and a converter project from n to n_n^{dc}. For two AC zones linked by at least one existing AC transmission project, create two candidate transmission projects, one AC on the original two zones, and one DC on the corresponding DC zones. This network construction is illustrated in Fig. 1. Let N^{ac}, N^{dc}, I^{ac}, I^{dc}, and I^{cv} denote the AC and DC zones, the AC and DC transmission projects, and the AC-DC converter projects. Then we have partitioned

979-8-3315-8138-1

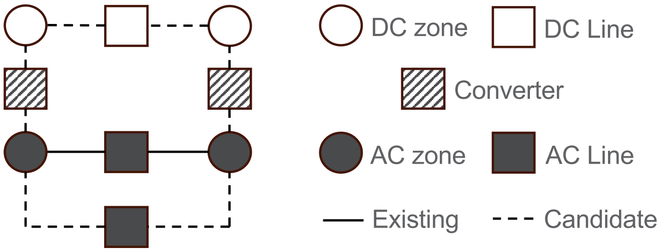

Fig. 1: Construction of network of zones and transmission projects: AC and DC zones. Existing AC, candidate AC, candidate DC, and candidate converter projects.

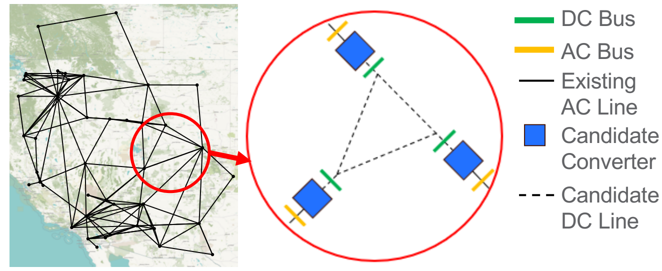

Fig. 2: Existing AC network with blow up of candidate DC and converter projects added.

N and I^{tr} as $N = N^{\text{ac}} \cup N^{\text{dc}}$ and $I^{\text{tr}} = I^{\text{ac}} \cup I^{\text{dc}} \cup I^{\text{cv}}$. And we have $n_i^{\text{fr}}, n_i^{\text{to}} \in N^{\text{ac}}$ for $i \in I^{\text{ac}}$, and $n_i^{\text{fr}}, n_i^{\text{to}} \in N^{\text{dc}}$ for $i \in I^{\text{dc}}$, while $n_i^{\text{fr}} \in N^{\text{dc}}$ for $i \in I^{\text{cv}}$, and $n_i^{\text{to}} \in N^{\text{ac}}$ for $i \in I^{\text{cv}}$.

C. Physics of Power Flow on AC and DC Links

In the basic CEP model, power flows p_{iyt} for $i \in I^{\text{tr}}$ are subject only to transmission capacity limits, without physical power flow laws. But in meshed AC and DC networks, Kirchhoff's laws determine the flows from nodal injections and line impedances. To approximate these physical laws tractably, CEP studies commonly adopt the DCPF formulation [20] for existing lines. We apply DCPF for $i \in I^{\text{ac}} \cup I^{\text{dc}}$, given resistance R_i and reactance X_i of a representative unit of project i. For $i \in I^{\text{ac}}$, assuming $R_i \ll X_i$, the operating admittance is $-u_{iy}^{\text{op}}/X_i$. Let θ_{nyt} be the variable voltage angle in AC zone n at time t in period y. Then p_{iyt} for $i \in I^{\text{ac}} \cap I^{\text{cand}}$ follows (9). For $i \in I^{\text{dc}} \cap I^{\text{cand}}$, we use a similar DCPF model in (10), assuming $X_i \ll R_i$, with a voltage magnitude variable v_{nyt} on DC zones n. Voltage magnitude is bounded in (11). For $i \in I^{\text{ac}} \cap I^{\text{ex}}$, we replace u_{iy}^{op} by fixed values $U_{iy}^{\text{ex,op}}$ in (12). Converter flows are modeled as controllable, with no flow law.

$$X_i p_{iyt} = u_{iy}^{\text{op}}(\theta_{nyt} - \theta_{n'yt}), \quad \forall i \in I^{\text{ac}} \cap I^{\text{cand}}, y \in Y, t \in T, n = n_i^{\text{fr}}, n' = n_i^{\text{to}} \tag{9}$$

$$R_i p_{iyt} = u_{iy}(v_{nyt} - v_{n'yt}), \quad \forall i \in I^{\text{dc}} \cap I^{\text{cand}}, y \in Y, t \in T, n = n_i^{\text{fr}}, n' = n_i^{\text{to}} \tag{10}$$

$$V_{nyt}^{\min} \leq v_{nyt} \leq V_{nyt}^{\max} \ \forall n \in N^{\text{dc}}, y \in Y, t \in T \tag{11}$$

$$X_i p_{iyt} = U_{iy}^{\text{op,ex}}(\theta_{nyt} - \theta_{n'yt}), \quad \forall i \in I^{\text{ac}} \cap I^{\text{cand}}, y \in Y, t \in T, n = n_i^{\text{fr}}, n' = n_i^{\text{to}} \tag{12}$$

D. Disjunctive formulation with binary investment

The quadratic expressions $u^{\text{op}}\theta$ and $u^{\text{op}}v$ in (9, 10) make the model a nonconvex quadratically constrained program (QCP). Nonconvex QCP solvers cannot guarantee global optimality or scale poorly in large instances. Therefore, we reformulate (9, 10) using only linear expressions by adding binary restrictions. The resulting disjunctive formulation is a MIP model, and MIP solvers give global optimality guarantees and scale well in practice. For this, we restrict u_{iy}^{op} to binary values for candidate AC and DC transmission projects in (13). Then we set linear constraints (14, 15), where $\theta_{nn'}^{\text{dmax}}$ and $V_{nn'}^{\text{dmax}}$ are the predetermined maximum angle and voltage differences between zones n and n'. Given (13), (14) is equivalent to (9), and (15) is equivalent to (10).

$$u_{iy}^{\text{op}} \in \{0,1\}, \forall i \in I^{\text{cand}} \cap (I^{\text{ac}} \cup I^{\text{dc}}), y \in Y \tag{13}$$

$$|X_i p_{iyt} - (\theta_{nyt} - \theta_{n'yt})| \leq \theta_{nn'}^{\text{dmax}}(1 - u_{iy}^{\text{op}}), \quad \forall i \in I^{\text{ac}} \cap I^{\text{cand}}, y \in Y, t \in T, n = n_i^{\text{fr}}, n' = n_i^{\text{to}} \tag{14}$$

$$|R_i p_{iyt} - (v_{nyt} - v_{n'yt})| \leq V_{nn'}^{\text{dmax}}(1 - u_{iy}^{\text{op}}), \quad \forall i \in I^{\text{dc}} \cap I^{\text{cand}}, y \in Y, t \in T, n = n_i^{\text{fr}}, n' = n_i^{\text{to}} \tag{15}$$

III. Large Scale Case Study

A. Simulation Setup

The proposed model is demonstrated using a system topology based on the Western Electricity Coordinating Council (WECC) 2030 Anchor Data Set (ADS) [21]. To reduce computational complexity, generation and transmission are aggregated to a 43-zone system [18]. AC candidate transmission is modeled in parallel with every existing AC line. We extend the topology of [18] by superimposing a candidate DC network on the AC network (i.e., one DC candidate parallel to each AC path), using the construction from section II-C. The DC candidate network connects to the AC network via candidate converters, each connecting an AC zone to its corresponding DC zone. The AC network, with detail of the candidate DC and converter projects, is shown in Fig. 2. We assume continuous investment for converters, and binary investment for AC and DC lines. DC line costs and capacities are taken from [22], while AC line costs and capacities are derived from [23].

We consider two load scenarios, business-as-usual growth (BAU), and high load growth due to the integration of large electric loads like data centers (LEL). For BAU, we first present results with only AC transmission investment (BAU-AC), followed by results that include both AC and MTDC investment (BAU-MTDC). We modeled one investment year (2040) and 360 operating hours comprising 24 hours across each 15 representative days.

Loads are based on multi-sector base-load projections [24]. For the LEL scenario, we supplement these projections with a 15% annual data-center load growth assumption from [25]. These loads were downscaled to the county level using population weighting and assigned an hourly profile by assuming a flat 8,760-hour data-center load. The hourly county-level loads

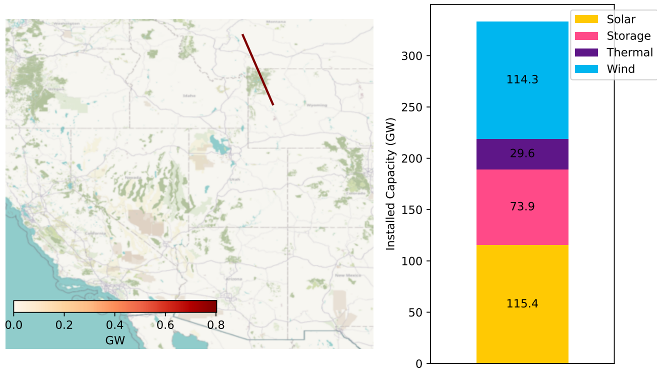

(a) BAU-AC

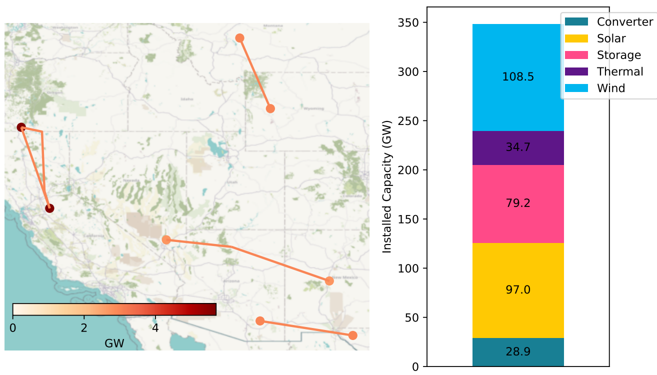

(b) BAU-MTDC

Fig. 3: BAU scenarios: Transmission and generation build.

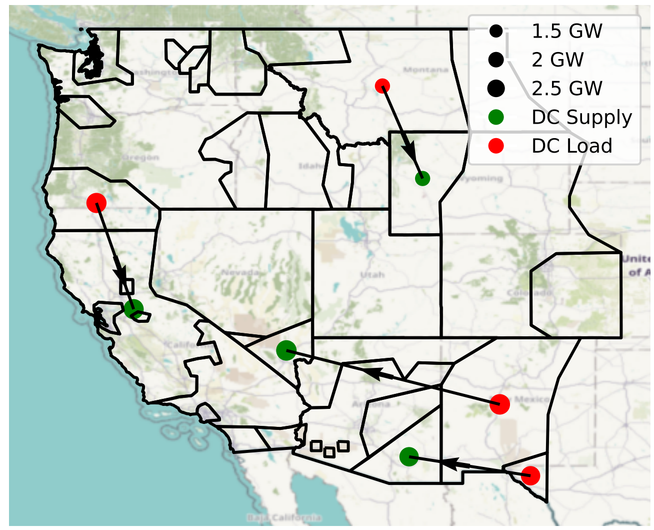

Fig. 4: BAU-MTDC scenario: Average converter injection or withdrawal and direction of DC energy transfer.

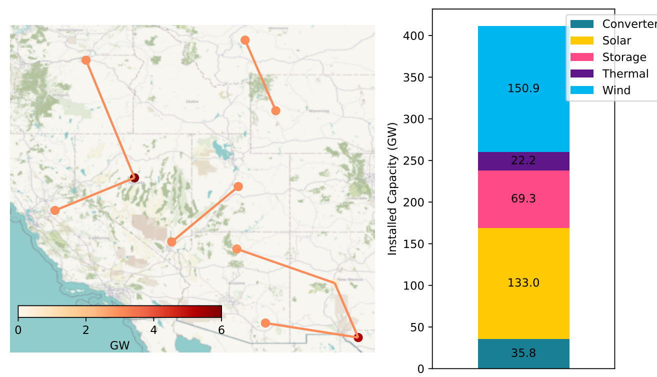

Fig. 5: LEL base scenario: Transmission and generation build.

were then aggregated to the 43 zones of our system model and sampled at the selected operating time points.

B. Effect of AC vs. DC Transmission Investment

Investments in transmission and generation with and without MTDC are shown in Fig. 3. When only AC transmission expansion is allowed (Fig. 3a), the model builds a single new line. By comparison, when MTDC candidate lines are available (Fig. 3b), the same corridor is built but as DC instead of AC, and several more DC lines are constructed. In addition, significantly less investment is made in solar and wind, suggesting that the availability of MTDC options allows better spatial coordination of new and existing resources. To this point, the annual delivered generation from wind and solar decreases by only 6.1 TWh (0.7%) despite capacity decreasing by 24.2 GW (10.5%), demonstrating lower curtailment and better utilization of energy. In turn, investment in conventional generation and storage increases, likely to serve local reliability needs. The total cost of investment and operation is 4% lower in BAU-MTDC than in LEL-AC.

Fig. 3b also shows the link selection and converter sizing results of the BAU-MTDC scenario. Both point-to-point (e.g., the line connecting Montana and Wyoming) and radial configurations are selected (e.g., the line connecting Nevada-Arizona-New Mexico). By optimizing converter capacity independently of transmission lines—instead of requiring converters on both ends of each DC link sized equal to the link capacity—the model avoids nearly 20 GW of converter capacity. This results in approximately $1.1 billion in savings (0.5%), underscoring the importance of dynamically selecting network configurations.

Source–sink relationships in Fig. 4 are indicated by the average injection or withdrawal at each converter, identifying whether the converter functions as a load or a supply within its AC zone. The lines illustrate the direction of energy transfer, generally flowing from remote supply regions to major load centers (e.g., Las Vegas and the San Francisco Bay Area).

C. DC Transmission Investment for Large Electric Loads

Generation and transmission expansion decisions for the LEL scenario are shown in Fig. 5. Inclusion of LEL not only increases the total load but also impacts the spatial distribution of load. In response, the model builds more variable generation, more converter capacity, and more (and different) transmission. Still, transmission is built in similar corridors in

979-8-3315-8138-1

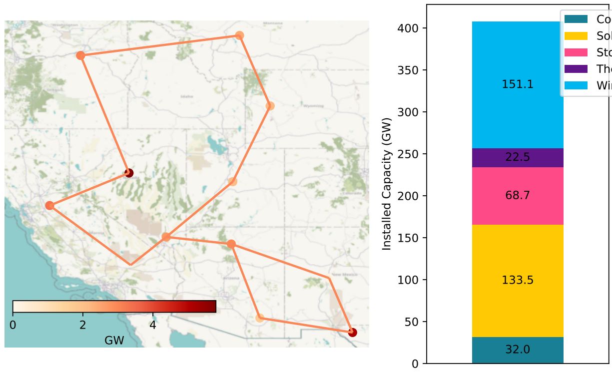

Fig. 6: LEL forced mesh scenario: Transmission and generation build.

the BAU and LEL scenarios, particularly along the Southwest, California-Oregon, and the Plains.

Fig. 6 shows results from a case with fixed transmission investment, building the DC links selected in the base LEL scenario, augmented to form a meshed MTDC network. This meshed MTDC network incurs a modest increase in cost of $1.3 billion (0.46%) relative to the $280.4 billion cost of the base LEL scenario. Meshed networks can have stability and reliability advantages not captured in our model, and this experiment illustrates the potential cost premium associated with pursuing those benefits.

IV. Conclusion

This paper introduced a CEP model that supports MTDC investment and allows independent selection of DC lines and sizing of converters. This capability enables the optimization of system configuration, including point-to-point, radial, and meshed layouts. Power flow physics is represented for AC and DC networks to capture operational limits and the flexibility provided by converters. The model is applied to a 43-zone system representing the Western Interconnection based on the WECC 2030 ADS. Simulation results show that DC investment out-competes AC and reduces the need for new variable generation capacity through more efficient utilization of new and existing resources. The LEL case demonstrates the additional value of MTDC transmission under high load growth. Further, evaluation of a large-scale meshed MTDC network suggested that such a reliability-enhancing configuration adds only modest system cost. Future work includes enabling continuous investment in transmission projects, and addressing the computational difficulty of the CEP problem with MTDC investment by developing heuristic solver algorithms and using more efficient power flow formulations.

References

[1] Q. Nguyen, H. Li, P. Etingov, M. Elizondo, J. Zhu, and X. Ke, "Benefits of Multi-Terminal HVdc Under Extreme Conditions via Production Cost Modeling Analyses," *IEEE Open Access J. Power Energy*, vol. 11, pp. 117–129, 2024.

[2] M. Barragan, et al., "Operational benefits of multiterminal dc-links in active distribution networks," in *Proc. IEEE Power Energy Soc. Gen. Meeting*, 2012, pp. 1–6.

[3] E. Schweitzer, K. Harris, K. Oikonomou, and N. Samaan, "Nodal Design of a US-Wide MTDC Overlay in Production Cost Modeling Using Industry Planning Cases," in *Proc. IEEE Power Energy Soc. Gen. Meeting*, 2025, pp. 1–5.

[4] K. Meah and S. Ula, "Comparative evaluation of HVDC and HVAC transmission systems," in *Proc. IEEE Power Eng. Soc. Gen. Meeting*, 2007, pp. 1–5.

[5] US DOE ARPA-E, "U.S. Department of Energy Announces $38 Million to Develop Next-Generation Transmission Infrastructure," November 2024. [Online]. Available: https://arpa-e.energy.gov/news-and-events/news-and-insights/us-department-energy-announces-38-million-develop-next-generation-transmission-infrastructure

[6] M. Moradi-Sepahvand and T. Amraee, "Hybrid AC/DC Transmission Expansion Planning Considering HVAC to HVDC Conversion Under Renewable Penetration," *IEEE Trans. Power Syst.*, vol. 36, no. 1, pp. 579–591, 2021.

[7] A. Lotfjou, Y. Fu, and M. Shahidehpour, "Hybrid AC/DC Transmission Expansion Planning," *IEEE Trans. Power Deliv.*, vol. 27, no. 3, pp. 1620–1628, 2012.

[8] L. M. Castro and N. González-Cabrera, "Short-term generation capacity expansion planning considering multi-terminal VSCHVDC links using a linear programming framework improved by shift factors," *Electric Power Systems Research*, vol. 206, p. 107819, 2022.

[9] A. H. Dominguez, L. H. Macedo, A. H. Escobar, and R. Romero, "Multistage Security-Constrained HVAC/ HVDC Transmission Expansion Planning With a Reduced Search Space," *IEEE Trans. Power Syst.*, vol. 32, no. 6, pp. 4805–4817, 2017.

[10] Z. Zhuo, et al., "Transmission Expansion Planning Test System for AC/DC Hybrid Grid With High Variable Renewable Energy Penetration," *IEEE Trans. Power Syst.*, vol. 35, no. 4, pp. 2597–2608, 2020.

[11] P. A. Bhattiprolu and A. J. Conejo, "Multi-Period AC/DC Transmission Expansion Planning Including Shunt Compensation," *IEEE Trans. Power Syst.*, vol. 37, no. 3, pp. 2164–2176, 2022.

[12] K. Meng, W. Zhang, J. Qiu, Y. Zheng, and Z. Y. Dong, "Offshore Transmission Network Planning for Wind Integration Considering AC and DC Transmission Options," *IEEE Trans. Power Syst.*, vol. 34, no. 6, pp. 4258–4268, 2019.

[13] A. Bloom, et al., "The Value of Increased HVDC Capacity Between Eastern and Western U.S. Grids: The Interconnections Seam Study," *IEEE Trans. Power Syst.*, vol. 37, no. 3, pp. 1760–1769, 2022.

[14] US DOE GDO, "The National Transmission Planning Study," Tech. Rep., 2024. [Online]. Available: https://www.energy.gov/gdo/national-transmission-planning-study

[15] NREL, "Model documentation - ReEDS 2.0," October 2025. [Online]. Available: https://nrel.github.io/ReEDS-2.0/model_documentation.html

[16] A. L. Figueroa-Acevedo, "Opportunities and benefits for increasing transmission capacity between the us eastern and western interconnections," Doctoral Dissertation, Iowa State University, 2017.

[17] J. T. Holzer, et al., "Grid Expansion Optimal Planning Tools (GridEO): Manual for Users and Developers," PNNL, Tech. Rep., 2024. [Online]. Available: https://www.osti.gov/biblio/2483837

[18] K. Oikonomou, et al., "Energy storage planning for enhanced resilience of power systems against wildfires and heatwaves," *J. Energy Storage*, vol. 119, p. 116074, 2025.

[19] T. V. Zuluaga, et al., "PTDF Power Flow for Stochastic Nodal Expansion Planning," https://www.ferc.gov/media/ptdf-powerflow-representation-accelerating-large-scale-stochastic-nodal-capacity-expansion, July 2025, accessed: 2025-09-25.

[20] A. Wood, B. Wollenberg, and G. Sheblé, *Power Generation, Operation, and Control*. Wiley, 2013.

[21] WECC, "2030 ADS PCM Release Notes," 2021. [Online]. Available: https://www.wecc.org/Reliability/2030ADS_PCM_ReleaseNotes_GV-V2.3_6-9-2021.pdf

[22] Midcontinent Independent System Operator, "Transmission Cost Estimation Guide for MTEP24," MISO, Tech. Rep., May 2024.

[23] R. Pletka, J. Khangura, A. Rawlins, E. Waldren, and D. Wilson, "Capital costs for transmission and substations," Western Electricity Coordinating Council, Tech. Rep., Feb. 2014.

[24] C. D. Burleyson, et al., "When do different scenarios of projected electricity demand start to meaningfully diverge?" *Appl. Energy*, vol. 380, p. 124948, 2025.

[25] EPRI, "Powering Intelligence: Analyzing Artificial Intelligence and Data Center Energy Consumption," https://www.epri.com/research/products/000000003002028905, May 2024.

979-8-3315-8138-1